JPE 1-1-4

Carrier Based SVPWM Method for Multi-Level System Considering Harmonic Distortion Factor

Yo-Han Lee*, Dong-Hyun Kim, and Dong-Seok Hyun

Hanyang University, Seoul 133-791 Korea

ABSTRACT

In most inverter/converter applications SVPWM method is a preferred approach since it shows good characteristics in linear modulation range and waveform quality. In this paper, we propose a new carrier based SVPWM method for multi-level system. First, we survey the conventional carrier based SVPWM method, and investigate the problem of the conventional one for the multi-level system with the focus on the switching frequency harmonic flux trajectories. Finally, we propose a new carrier based SVPWM method that can reduce harmonic distortion. Simulation and experimental results are given for verification of the proposed SVPWM method.

Key Words : carrier based SVPWM, harmonic distortion, harmonic flux trajectories, multi-level system

1. Introduction

Carrier based PWM methods employ the 'per carrier cycle volt-second balance' principle to program a desirable inverter output voltage waveform. In most three-phase AC motor drive and utility interface applications, the neutral point of load is isolated and no neutral current path exists. In such applications, any zero sequence signal can be injected to the reference modulation waves. A properly selected zero sequence signal can extend the linear modulation range of sinusoidal PWM (SPWM). Furthermore, it can improve the waveform quality, that is to say, harmonic distortion can be reduced significantly [1-3].

Recognizing this property, many researchers have been investigating the zero sequence signal dependency of the modulator performance and a large number of PWM methods with unique characteristics have been reported[2], [4-7]. With the injection of the zero sequence signal, partition of zero voltage vectors is changed, and it has an effect on the waveform quality. Of those PWM methods, the space vector PWM (SVPWM) method shows good characteristics in waveform quality. It has equally divided zero voltage vectors, by which the harmonic distortion can be reduced.

In case of multi-level system[8-9], there are many output vectors and voltage level increases the complexity of SVPWM. Therefore, the carrier based SVPWM with triangular intersection technique is necessary for multi-level applications [10].

Conventional carrier based SVPWM for multi-level system shows good characteristics in linear modulation range. However, it is distinguished from the SVPWM method for 2-level system in that not only it splits non-zero voltage vectors, but also it has unequally divided

* Corresponding author
Tel. : +82-2-2290-0341
Fax. : +82-2-2297-1569
E-mail : johnlee@ihanyang.ac.kr

voltage vectors.

In general, harmonic distortion analysis can be done by either harmonic distortion factor[2] or FFT results. Both analyses show similar results for the waveform quality. Harmonic distortion factor (HDF), however, is more suitable for quantitative analysis.

This paper first reviews the conventional carrier based SVPWM, and explains a problem when the conventional carrier based SVPWM is used for multi-level system based on harmonic flux trajectory analysis. The remainder of the paper is dedicated to the development of the new carrier based SVPWM method. HDF analysis will show that the proposed SVPWM has lower HDF than the conventional one. Simulation results and experimental results will show the effectiveness of the proposed SVPWM method.

2. Comparison of carrier based PWM methods for 2-level system

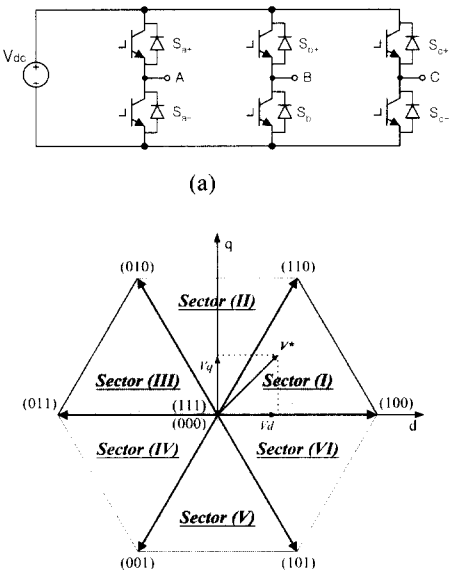

(a)

(b)

Fig. 1. The circuit diagram and the space vector diagram of 2-level inverter system : (a) circuit diagram , (b) space vector diagram (b).

In case of 2-level system, the most popular PWM modulators are SPWM, SVPWM, THIPWM1/4, THIPWM1/6, DPWM0, DPWM1, DPWM2 and

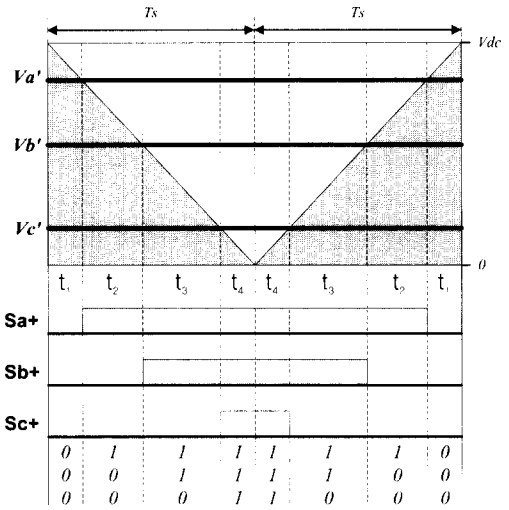

Fig. 2. The per carrier cycle view of switching signals and the output voltage vectors of sector (I) for SVPWM method (2-level).

DPWM3 [3]. Generally, they are divided into two groups according to the modulator characteristics: 1) continuous PWMs (CPWMs) 2) discontinuous PWMs (DPWMs). The CPWMs are also subdivided into two groups: 1) SPWM 2) SVPWM, THIPWM1/4, THIPWM1/6. Each group shows similar characteristics. Of those PWM methods, the SVPWM shows good characteristics in overall performance such as linear modulation range and waveform quality.

Fig. 1 shows the circuit diagram and the space vector diagram of 2-level system. SVPWM method can be summarized as follows [10].

The command voltages V_d, V_q are converted to imaginary phase voltages V_a, V_b, V_c, as is (1). After calculating zero sequence voltage as is (2), the effective phase voltages V_a`, $V_b$`, V_c` can be obtained by (3).

$$\begin{aligned} V_a &= V_d \\ V_b &= -1/2 \cdot V_d + \sqrt{3}/2 \cdot V_q \\ V_c &= -1/2 \cdot V_d - \sqrt{3}/2 \cdot V_q \end{aligned} \tag{1}$$

$$V_{shift} = \frac{1}{2} V_{dc} - \frac{1}{2}(V_{\max} + V_{\min}) \tag{2}$$

where, V_{max} is the largest voltage among V_a, V_b, V_c and V_{min} is the smallest one among V_a, V_b, V_c.

$$V_x' = V_x + V_{shift}(x = a,b,c) \tag{3}$$

If the effective phase voltages are compared with triangular carrier wave, the gating signals are generated.

Fig. 2 shows the per carrier cycle view of switching signals and output voltage vectors of sector (I) for SVPWM method. As we can see from the figure, the zero voltage vectors *(0, 0, 0)* and *(1, 1, 1)* have the same switching time.

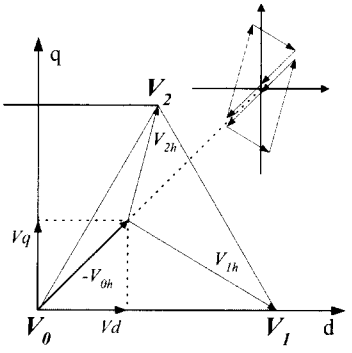

Fig. 3. The HFT in the sector (I) for SVPWM method (2-level).

Fig. 3 shows the examples of the harmonic flux trajectories (HFT) for SVPWM method according to the command voltage vector. As illustrated in Fig. 3, within each cycle the harmonic voltage vectors V_{1h}, V_{2h} and V_{0h} are space and modulation index dependent. Here, the position of the command vector (θ) and the modulation index (k) is defined as follows :

$$\theta = \pi\left(\frac{V_d - |V_d|}{2 \cdot V_d}\right) + \tan^{-1}\left(\frac{V_q}{V_d}\right) \tag{4}$$

$$k = \frac{\sqrt{V_d^{\,2} + V_q^{\,2}}}{Vdc/\sqrt{3}} \tag{5}$$

The harmonic flux in the N'th cycle is calculated in the following :

$$\lambda(k,\theta) = \int_{NTs}^{(N+1)Ts} (V_m - V^*)dt \tag{6}$$

In the above formula, V_m is the inverter output voltage vector of the m'th state and within the carrier cycle it changes according to the selected switching sequence. And the per carrier cycle RMS value of the harmonic flux can be calculated as follows :

$$\lambda^2_{RMS} = \int_0^1 \lambda^2 \, dt \tag{7}$$

Since popular PWM methods have sixfold space symmetry, the per fundamental cycle RMS harmonic flux value can be calculated in the following.

$$HDF = \frac{1}{\pi/3}\int_0^{\pi/3} \lambda^2_{RMS} d\theta \tag{8}$$

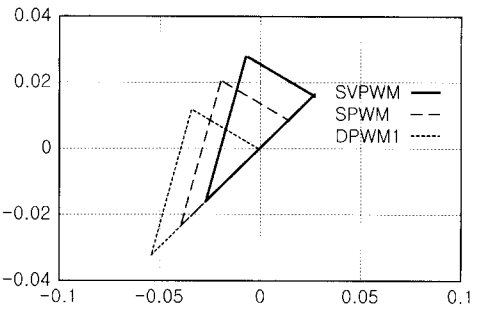

Fig. 4. An example of the switching frequency HFT of some PWM methods when $\theta=\pi/4$, k=0.6.

Fig. 4 shows an example of the switching frequency HFT of SVPWM, SPWM, and DPWM1, respectively. Since the distance to the origin is equal to the magnitude of the harmonic flux, the trajectories which are closer to the origin result in smaller harmonic flux and the per carrier cycle RMS flux value decreases. Generally, SVPWM has the smaller harmonic flux, for it splits the zero voltage vectors equally, which is important characteristic of SVPWM.

3. Improved carrier-based SVPWM for multi-level System

First of all, we explain 3-level system, and extend it to the multi-level system. Fig. 5 shows the HDF curves of 3-level system (see appendix A) in the linear modulation range under constant carrier frequency, which is similar to those of the 2-level system [3].

From the fig. 5, we can see that the SVPWM shows

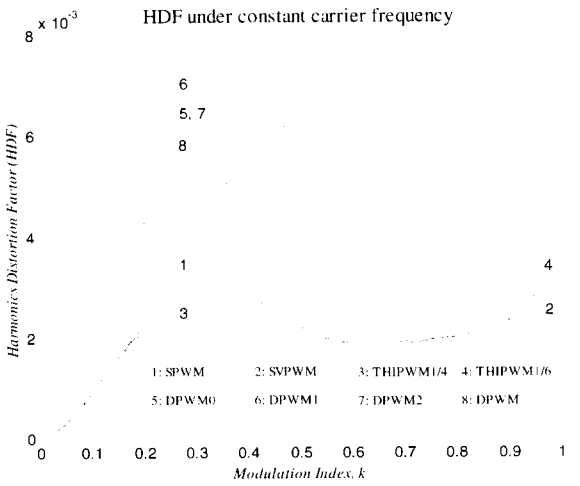

Fig. 5. HDF curves in the linear modulation range under constant carrier frequency (3-level).

good performance in HDF. Although THIPWM1/4 method is minimum harmonic distortion method in some range, it has only slightly less distortion than that of SVPWM and it is difficult to be realized.

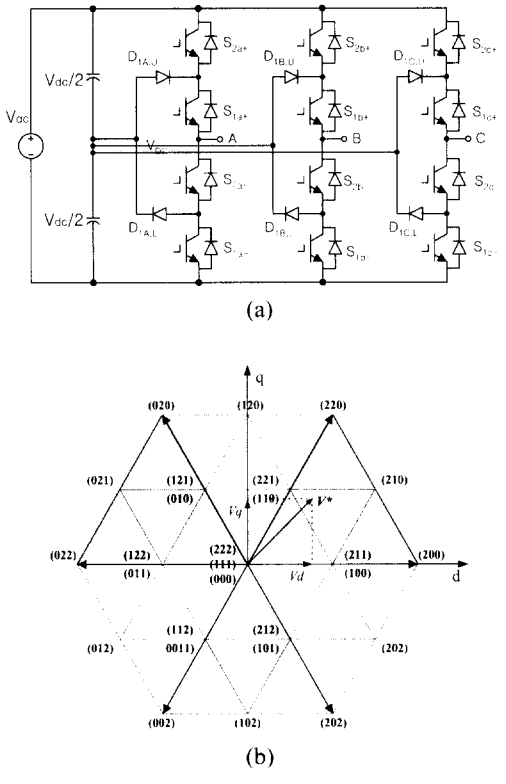

Fig. 6. The circuit diagram and the space vector diagram of 3-level system : (a) circuit diagram, (b) space vector diagram.

As DPWMs have fewer switching frequencies under constant carrier frequency, they may have smaller HDF than SVPWM in some points under the same switching frequency. But, DPWM are not suitable for NPC-type multi-level system.

SVPWM may be regarded as the best choice for multi-level system considering HDF. From now on, let's review conventional SVPWM for 3-level system briefly.

Fig. 6 shows the circuit diagram and the space vector diagram for the 3-level system. SVPWM method for the 3-level is equal to those of the 2-level system with the exception of two carrier waves. If the effective phase voltages are compared with two triangular carrier waves whose phase and magnitude are identical (only when the carrier waves of the same phase are used, the nearest three voltage vectors are selected) and whose frequency is $1/(2Ts)$, the gating signals can be generated.

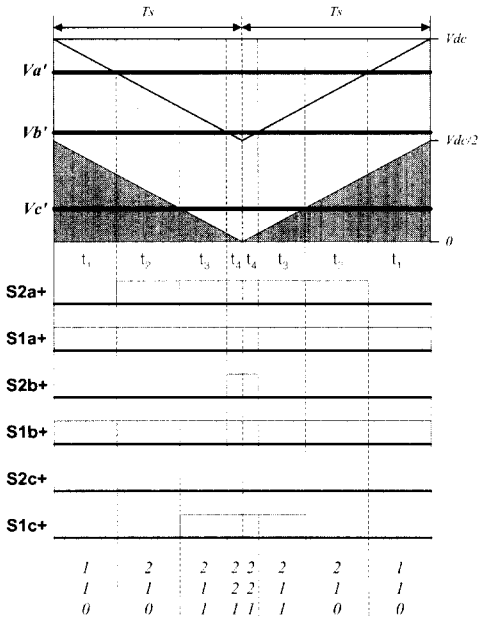

Fig. 7. The per carrier cycle view of switching signals and the output voltage vectors of sector (I) for SVPWM method (3-level).

Fig. 7 shows the per carrier cycle view of switching signals and output voltage vectors of sector (I) for SVPWM method. Fig. 8 shows examples for the HFT according to the command voltage vector (compare it with fig. 3).

Comparing fig. 2 and 3 with fig. 7 and 8, we can see

the difference between SVPWM of 2-level and 3-level system. First, in case of 2-level, the zero voltage vectors exist in the start-point/end-point of the sampling time, whereas in case of 3-level, the small voltage vectors exist. Second, in case of 2-level, it splits the zero voltage vectors equally, whereas in case of 3-level, it splits the small voltage vectors unequally (in case of NPC-type multi-level system, partition of small voltage vectors is related with dc-link voltage balancing, which will not be discussed in this paper). Therefore, for smaller harmonic flux, additional zero sequence signal should be added so as to split the small voltage vectors equally.

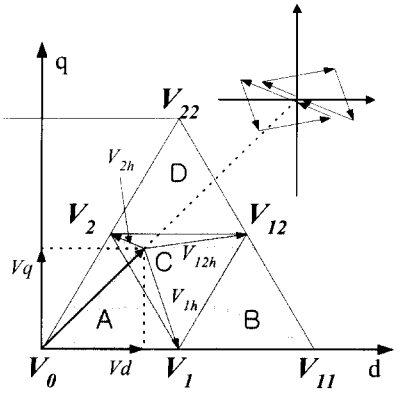

Fig. 8. The HFT in the sector (I) for conventional SVPWM method (3-level).

A simple sequence to get an additional zero sequence voltage is shown in fig. 9.

Fig. 9 (a) shows the effective phase voltages for the conventional SVPWM method. First, the effective phase voltages which are larger than Vdc/2 are shifted by –Vdc/2 as shown in fig. 9 (b). The shifted phase voltages can be calculated as follows :

$$V_x'' = V_x' \bmod \frac{V_{dc}}{n-1} (x = a,b,c) \tag{9}$$

where, *mod* means the remainder after division, and n denotes voltage level.

Second, an additional zero sequence voltage is added to the shifted phase voltages, as shown in fig. 9 (c). It can be calculated as follows :

$$V_{add\_shift} = \frac{1}{2(n-1)} V_{dc} - \frac{1}{2}(V_{\max}' + V_{\min}') \tag{10}$$

where, V_{max}' is the largest voltage among V_a'', V_b'', V_c'', and V_{min}' is the smallest one among V_a'', V_b'', V_c''.

Finally, the effective phase voltages which were shifted by –Vdc/2 are shifted by +Vdc/2, as shown in fig. 9 (d). As a result, the small voltage vectors are divided into equally, by which the harmonic distortion can be reduced.

The proposed method can be easily extended to multi-level system with similar manner.

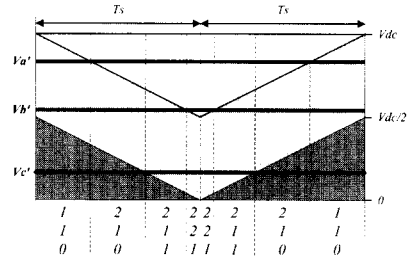

(a) original state

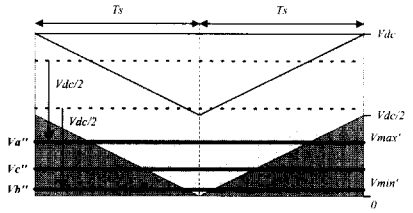

(b) 1st sequence

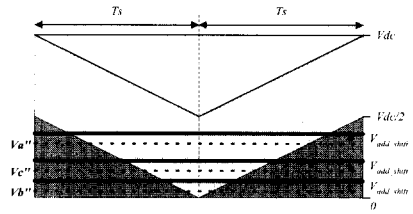

(c) 2nd sequence

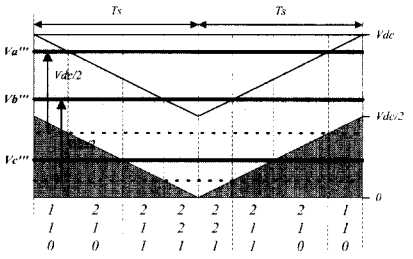

(d) 3rd sequence

Fig. 9. The sequence to get an additional zero sequence voltage.

HDF curve of the proposed SVPWM for the 3-level system is shown in fig. 10. As we can see from the results, proposed SVPWM method shows better performance than the conventional SVPWM method.

Fig. 11 and 12 show the simulation results for the 3-level and 4-level system, respectively. The simulation conditions are as follows: f=50[Hz], Ts=666.6[us], Vdc=300[V].

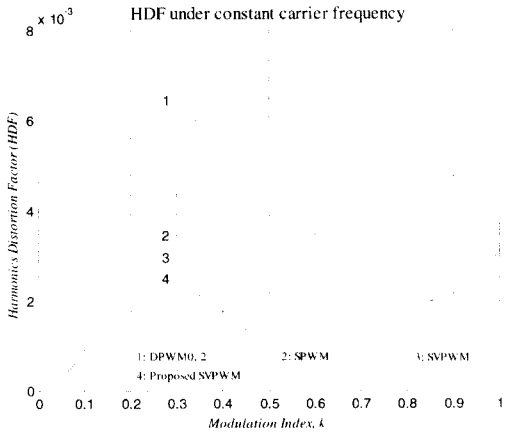

Fig. 10. HDF curves in the linear modulation range under constant carrier frequency (3-level).

Command phase voltage, line-to-line voltage, FFT results are given for k=0.2, k=0.5, and k=0.8, respectively. In the figure, (a), (c) and (e) are the cases with the conventional method and (b), (d) and (f) are the cases with the proposed method. The proposed SVPWM method for the 3-level system shows good results in FFT analysis. However, in case of k=0.8, the FFT result of the proposed SVPWM shows little difference, as we can see from HDF curves in fig. 10. In case of 4-level system, the proposed SVPWM also shows good results in FFT analysis (though the exactly same output is acquired when k<1/3).

Fig. 13 shows the experimental results.

The experimental conditions are as follows: f=50[Hz], Ts=250[us], Vdc=310[V].

Command phase voltage, line-to-line voltage, FFT results are given for k=0.2, k=0.5, and k=0.8, respectively. When k=0.8, for the modulation wave of the conventional SVPWM is similar to those of the proposed SVPWM, the FFT results shows little difference.

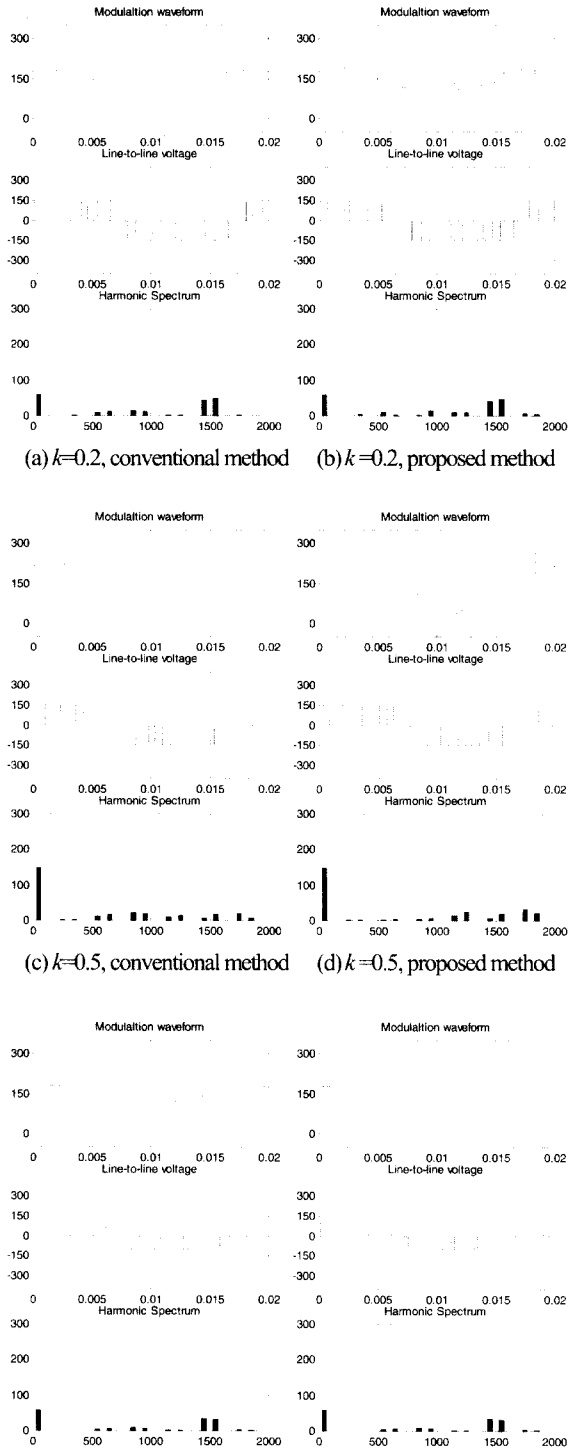

(a) k=0.2, conventional method (b) k=0.2, proposed method

(c) k=0.5, conventional method (d) k=0.5, proposed method

(e) k=0.8, conventional method (f) k=0.8, proposed method

Fig. 11. Simulation results for the 3-level system. The effective phase voltage, output line-to-line voltage, and FFT results ; (a), (c) and (e) : conventional method. (b), (d) and (f) : proposed method.

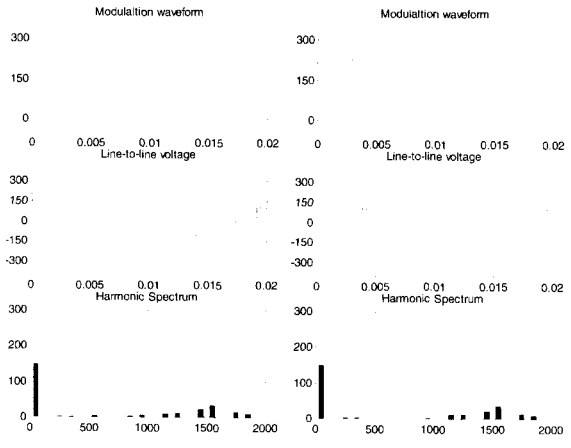

(a) k=0.2,conventional method (b) k=0.2, proposed method

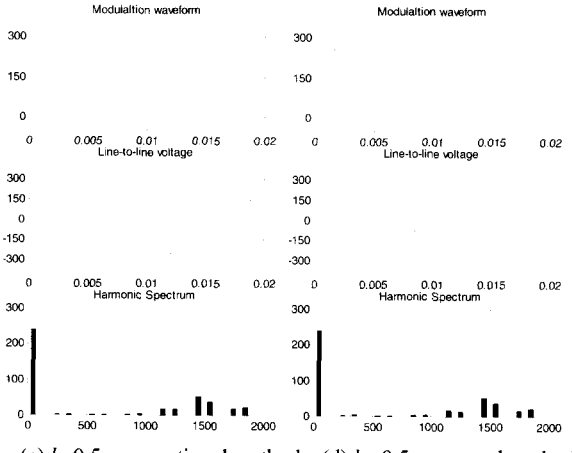

(c) k=0.5, conventional method (d) k =0.5, proposed method

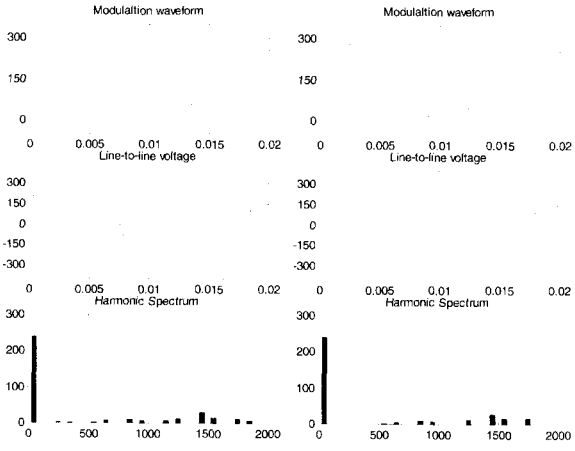

(e) k=0.8, conventional method (f) k =0.8, proposed method

Fig. 12. Simulation results for the 4-level system. The effective phase voltage, output line-to-line voltage, and FFT results ; (a), (c) and (e) : conventional method. (b), (d) and (f) : proposed method.

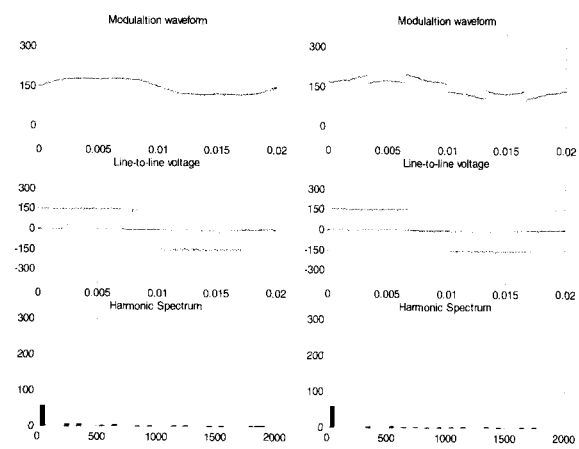

(a) k=0.2, conventional method (b) k =0.2, proposed method

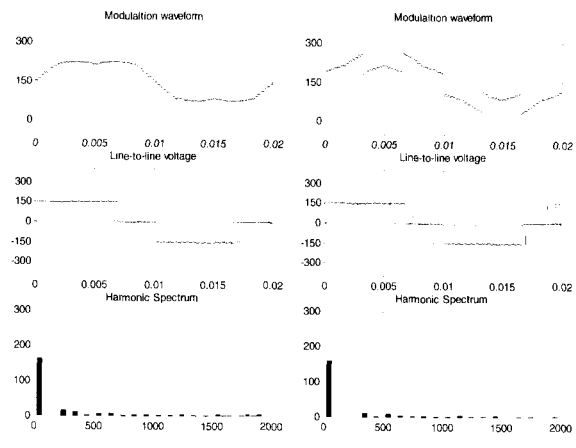

(c) k=0.5, conventional method (d) k =0.5, proposed method

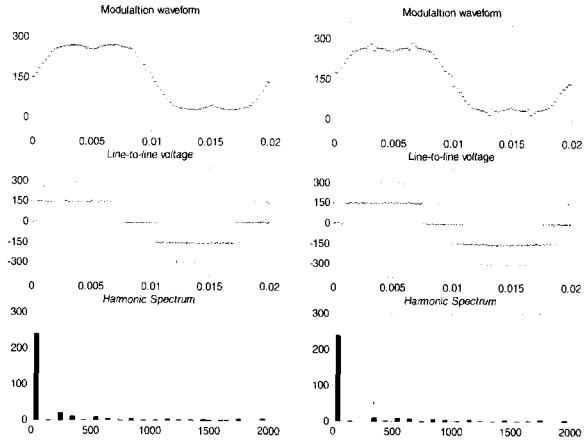

(e) k=0.8, conventional method (f) k =0.8, proposed method

Fig. 13. Experimental results for the 3-level system. The effective phase voltage, output line-to-line voltage, and FFT results ; (a), (c) and (e) : conventional method. (b), (d) and (f) : proposed method.

4. Conclusion

Because the multi-level system increase the complexity of SVPWM method, the carrier based SVPWM with triangular intersection technique is necessary for multi-level applications. When we use conventional carrier based SVPWM in multi-level system, the linear modulation range is the same as the conventional one. However, the waveform quality is not so good for the unequally divided voltage vector.

In this paper, we briefly reviewed the conventional SVPWM method and investigated the problem with the focus on the switching frequency HFT when it is extended to multi-level system. To solve the problem we use additional zero sequence voltage command, by which HDF can be reduced. We presented a simple method to get an additional zero sequence signal for multi-level system. HFT analysis shows that the HDF of the proposed SVPWM method is superior to conventional one. And simulation results and experimental results are given to verify the analysis.

References

[1] J. Holtz, "Pulsewidth modulation for electronic power conversion," *Proceedings of IEEE*, vol. 82. no. 3, pp. 1194~1214, 1994.

[2] A. M. Hava, R. J. Kerkman, and T. A. Lipo, "A high-performance generalized discontinuous PWM algorithm," *IEEE Trans. Ind. Applicat.*, vol. 34, no. 5 , pp. 1059 ~1071, Sept/Oct 1998.

[3] A. M. Hava, R. J. Kerkman, and T. A. Lipo, "Simple analytical and graphical methods for carrier-based PWM-VSI drives," *IEEE Trans. Power Electron.*, vol. 14, no. 1, 49~61, Jan 1999.

[4] J. A. Houldsworth and D. A. Grant, "The use of harmonic distortion to increase the output voltage of a three-phase PWM inverter," *IEEE Trans. Ind. Applicat.*, pp. 1224~1228, Sept/Oct. 1984.

[5] H. W. Van Der Broeck, H. Skudelny, and G. Stanke, "Analysis and realization of a pulse width modulator based on voltage space vectors," *IEEE Trans. Ind. Applicat.*, vol. 24, no. 1, pp. 142~150, Jan/Feb 1988.

[6] S. Ogasawara, H. Akagi, and A. Nabae, "A vovel PWM scheme of voltage source inverter based on space vector theory," in *Proc. EPE'89*, 1989, pp. 1197~1202.

[7] J. W. Kolar, H. Ertl, and F. C. Zach, "Minimization of the harmonics RMS values of three-phase PWM converter systems by optimal and suboptimal transition between continuous and discontinuous modulation," in *Proc. IEEE PESC'91*, 1991, pp. 372~381.

[8] P. M. Bhagwat and V. R. Stefanovic, "Generalized structure of a multilevel PWM inverter," *IEEE Trans. Ind. Applicat.*, vol. 19, no. 6, pp. 1057~1069, Nov/Dec 1983.

[9] J. S. Lai, and F. Z. Peng, "Multilevel converters-a new breed of power converters," *IEEE Trans. Ind. Applicat.*, vol. 32, no. 3, pp. 509~517, May/June 1996.

[10] Y. H. Lee, R. Y. Kim, and D. S. Hyun, "A novel SVPWM strategy for a multi-level voltage source inverter," in *Proc. IEEE APEC'99*, 1999, pp. 509~514.

Appendix A. Harmonic Flux Calculation.

Harmonic flux is dependent on the output sequence of the voltage vector and its time duration. In Table A, we summarize the sequence in case of 3-level system. Therefore, the harmonic flux in each region can be calculated in the following. HDF can be calculated by substituting it to (7).

Table A Output Sequence for the Sector (I)

	$0 \le \theta < \pi/6$	$\pi/6 \le \theta < \pi/3$
Region A	$V_{1-} \rightarrow V_{2-} \rightarrow V_0 \rightarrow V_{1+}$	$V_{2-} \rightarrow V_0 \rightarrow V_{1+} \rightarrow V_{2+}$
Region B	$V_{1-} \rightarrow V_{11} \rightarrow V_{12} \rightarrow V_{1+}$	
Region C	$V_{1-} \rightarrow V_2 \rightarrow V_{12} \rightarrow V_{1+}$	$V_{2-} \rightarrow V_{12} \rightarrow V_{1+} \rightarrow V_{2+}$
Region D	$V_{2-} \rightarrow V_{12} \rightarrow V_{22} \rightarrow V_{2+}$	

V_{1-} : (1 0 0) V_{1+} : (2 1 1) V_{2-} : (1 1 0) V_{2+} : (2 2 1)

A-1. Region A ($0 \le \theta < \pi/6$)

① $0 \le t < t_1$

$$\lambda = (\frac{1}{\sqrt{3}} - ke^{j\theta})t$$

② $t_1 \le t < t_1+t_2$

$$\lambda = (\frac{1}{\sqrt{3}}e^{j\pi/3} - ke^{j\theta})t + (\frac{1}{\sqrt{3}} - \frac{1}{\sqrt{3}}e^{j\pi/3})t_1$$

③ $t_1+t_2 \le t < t_1+t_2+t_3$

$$\lambda = -ke^{j\theta}t + \frac{1}{\sqrt{3}}t_1 + \frac{1}{\sqrt{3}}e^{j\pi/3}t_2$$

④ $1-t_4 \le t < 1$

$$\lambda = (\frac{1}{\sqrt{3}} - ke^{j\theta})t - \frac{1}{\sqrt{3}} + \frac{1}{\sqrt{3}}t_1 + \frac{1}{\sqrt{3}}e^{j\pi/3}t_2 + \frac{1}{\sqrt{3}}t_4$$

A-2. Region A ($\pi/6 \le \theta < \pi/3$)

① $0 \le t < t_1$

$$\lambda = (\frac{1}{\sqrt{3}} e^{j\pi/3} - ke^{j\theta})t$$

② $t_1 \le t < t_1+t_2$

$$\lambda = -ke^{j\theta}t + \frac{1}{\sqrt{3}} e^{j\pi/3} t_1$$

③ $t_1+t_2 \le t < t_1+t_2+t_3$

$$\lambda = (\frac{1}{\sqrt{3}} - ke^{j\theta})t - \frac{1}{\sqrt{3}}(t_1+t_2) + \frac{1}{\sqrt{3}} e^{j\pi/3} t_1$$

④ $1\text{-}t_4 \le t < 1$

$$\lambda = (\frac{1}{\sqrt{3}} e^{j\pi/3} - ke^{j\theta})t - \frac{1}{\sqrt{3}} e^{j\pi/3} + \frac{1}{\sqrt{3}} e^{j\pi/3} t_4 + \frac{1}{\sqrt{3}} e^{j\pi/3} t_1 + \frac{1}{\sqrt{3}}$$

A-3. Region B

① $0 \le t < t_1$

$$\lambda = (\frac{1}{\sqrt{3}} - ke^{j\theta})t$$

② $t_1 \le t < t_1+t_2$

$$\lambda = (\frac{2}{\sqrt{3}} - ke^{j\theta})t - \frac{1}{\sqrt{3}} t_1$$

③ $t_1+t_2 \le t < t_1+t_2+t_3$

$$\lambda = (e^{j\pi/6} - ke^{j\theta})t + (\frac{1}{\sqrt{3}} - e^{j\pi/6})t_1 + (\frac{2}{\sqrt{3}} - e^{j\pi/6})t_2$$

④ $1\text{-}t_4 \le t < 1$

$$\lambda = (\frac{1}{\sqrt{3}} - ke^{j\theta})t - \frac{1}{\sqrt{3}} + \frac{1}{\sqrt{3}} t_1 + \frac{2}{\sqrt{3}} t_2 + e^{j\pi/6} t_3 + \frac{1}{\sqrt{3}} t_4$$

A-4. Region C ($0 \le \theta < \pi/6$)

① $0 \le t < t_1$

$$\lambda = (\frac{1}{\sqrt{3}} - ke^{j\theta})t_1$$

② $t_1 \le t < t_1+t_2$

$$\lambda = (\frac{1}{\sqrt{3}} e^{j\pi/3} - ke^{j\theta})t + (\frac{1}{\sqrt{3}} - \frac{1}{\sqrt{3}} e^{j\pi/3})t_1$$

③ $t_1+t_2 \le t < t_1+t_2+t_3$

$$\lambda = (e^{j\pi/6} - ke^{j\theta})t - e^{j\pi/6}(t_1+t_2) + \frac{1}{\sqrt{3}} t_1 + \frac{1}{\sqrt{3}} e^{j\pi/3} t_2$$

④ $1\text{-}t_4 \le t < 1$

$$\lambda = (\frac{1}{\sqrt{3}} - ke^{j\theta})t - \frac{1}{\sqrt{3}} + \frac{1}{\sqrt{3}} t_1 + \frac{1}{\sqrt{3}} e^{j\pi/3} t_2 + e^{j\pi/6} t_3 + \frac{1}{\sqrt{3}} t_4$$

A-5. Region C ($\pi/6 \le \theta < \pi/3$)

① $0 \le t < t_1$

$$\lambda = (\frac{1}{\sqrt{3}} e^{j\pi/3} - ke^{j\theta})t$$

② $t_1 \le t < t_1+t_2$

$$\lambda = (e^{j\pi/6} - ke^{j\theta})t + \frac{1}{\sqrt{3}} e^{j\pi/3} t_1 - e^{j\pi/6} t_1$$

③ $t_1+t_2 \le t < t_1+t_2+t_3$

$$\lambda = (\frac{1}{\sqrt{3}} - ke^{j\theta})t + (\frac{1}{\sqrt{3}} e^{j\pi/3} - \frac{1}{\sqrt{3}})t_1 + (e^{j\pi/6} - \frac{1}{\sqrt{3}})t_2$$

④ $1\text{-}t_4 \le t < 1$

$$\lambda = (\frac{1}{\sqrt{3}} e^{j\pi/3} - ke^{j\theta})t - \frac{1}{\sqrt{3}} e^{j\pi/3} + \frac{1}{\sqrt{3}} e^{j\pi/3} t_4 + \frac{1}{\sqrt{3}} e^{j\pi/3} t_1 + \frac{1}{\sqrt{3}} t_3$$

A-6. Region D

① $0 \le t < t_1$

$$\lambda = (\frac{1}{\sqrt{3}} e^{j\pi/3} - ke^{j\theta})t$$

② $t_1 \le t < t_1+t_2$

$$\lambda = (e^{j\pi/6} - ke^{j\theta})t + (\frac{1}{\sqrt{3}} e^{j\pi/3} - e^{j\pi/6})t_1$$

③ $t_1+t_2 \le t < t_1+t_2+t_3$

$$\lambda = (\frac{2}{\sqrt{3}} e^{j\pi/3} - ke^{j\theta})t - \frac{1}{\sqrt{3}} e^{j\pi/3} t_1 + (e^{j\pi/6} - \frac{2}{\sqrt{3}} e^{j\pi/3})t_2$$

④ $1\text{-}t_4 \le t < 1$

$$\lambda = (\frac{1}{\sqrt{3}} e^{j\pi/3} - ke^{j\theta})t - \frac{1}{\sqrt{3}} e^{j\pi/3} + \frac{1}{\sqrt{3}} e^{j\pi/3} t_1 + e^{j\pi/6} t_2 + \frac{2}{\sqrt{3}} e^{j\pi/3} t_3 + \frac{1}{\sqrt{3}} e^{j\pi/3} t_4$$

Yo-Han Lee was born in 1970 in Seoul, Korea. He received the B. S. degree and M. S. degree from Hanyang University, in 1993 and 1995, respectively. He is now working toward Ph. D degree in the same university.

Dong-Hyun Kim was born in 1976 in Seoul, Korea. He received the B. S. degree and M. S. degree from Hanyang University, in 1999 and 2001, respectively. He is working at INTERPOWER Corporation.

Dong-Seok Hyun received the B.S. and M.S. degrees in electrical engineering from Hanyang University, Seoul, Korea, in 1973 and 1978, respectively, and the Ph.D. degree in electrical engineering from Seoul National University, Seoul, Korea, in 1986. From 1976 to 1979, he was with the Agency of Defense Development, Korea, as a Researcher.

He was a Research Associate in the department of Electrical Engineering, University of Toledo, Toledo, OH, from 1984 to 1985 and a Visiting Professor in the department of Electrical Engineering at the Technical University of Munich, Germany, from 1988 to 1989.

Since 1979, he has been with Hanyang University, where he is currently a Professor in the department of Electrical Engineering and Director of the Advanced Institute of Electrical Engineering and Electronics (AIEE). He is the author of more than 90 publications concerning electric machine design, high-power engineering, power electronics, and motor drives. His research interests include power electronics, motor drives, digital signal processing, traction, and their control systems. Dr. Hyun is a member of the IEEE Power Electronics, Industrial Electronics, Industry Applications, and Electron Devices Societies. He is also a member of the Institution of Electrical Engineers (U.K.), the Korean Institute of Power Electronics, and the Korean Institute of Electrical Engineers.